Helicity Induction and Its Static Memory of Poly(biphenylylacetylene)s Bearing Pyridine *N*-Oxide Groups and Their Use as Asymmetric Organocatalysts

Mitsuka Ando,[1] Ryoma Ishidate,[2] Tomoyuki Ikai,[1] Katsuhiro Maeda,[3,4] Eiji Yashima[1,2]

[1]Department of Molecular and Macromolecular Chemistry, Graduate School of Engineering, Nagoya University, Chikusa-ku, Nagoya 464-8603, Japan
[2]Department of Molecular Design and Engineering, Graduate School of Engineering, Nagoya University, Chikusa-ku, Nagoya 464-8603, Japan
[3]Graduate School of Natural Science and Technology, Kanazawa University, Kakuma-machi, Kanazawa 920-1192, Japan
[4]Nano Life Science Institute (WPI-NanoLSI), Kanazawa University, Kakuma-machi, Kanazawa 920-1192, Japan
Correspondence to: E. Yashima (E-mail: yashima@chembio.nagoya-u.ac.jp)

Received 31 July 2019; Revised 31 August 2019; accepted 5 September 2019
DOI: 10.1002/pola.29501

ABSTRACT: Novel poly(biphenylylacetylene) derivatives carrying different types of pyridine *N*-oxide units with a bulky or less-bulky substituent at a different position as the functional pendant groups (poly-**2a** and poly-**2b**) were synthesized by the rhodium-catalyzed polymerization of the corresponding monomers. The influence of the steric environment around the catalytically active pyridine *N*-oxide sites on the helicity induction and its static memory as well as the asymmetric catalytic activities of the resulting helical polymers with a macromolecular helicity memory was investigated. The polyacetylenes formed an excess one-handed helical conformation upon noncovalent interactions with optically active alcohols and the induced macromolecular helicities of the polyacetylenes were efficiently memorized after the removal of the chiral inducers. Poly-**2b** with the macromolecular helicity memory showed an enantioselectivity for the catalytic asymmetric allylation of benzaldehydes, producing optically active allyl alcohols, although their enantioselectivities were low. On the other hand, poly-**2a** exhibited a negligible catalytic activity probably due to the bulky substituent at the *o*-position of the pyridine *N*-oxide residues, while poly-**2a** underwent a unique helix-inversion with the increasing concentration of chiral alcohols and the opposite helicity of poly-**2a** was further successfully memorized. © 2019 Wiley Periodicals, Inc. J. Polym. Sci., Part A: Polym. Chem. **2019**

KEYWORDS: asymmetric polymer catalyst; biphenyl; helicity induction; memory; organocatalyst; polyacetylene

INTRODUCTION Inspired by the sophisticated functions of biological helical polymers and their assemblies, a rich variety of artificial helical polymers has been prepared over the past decades[1–8] in order to develop advanced chiral materials for the resolution of enantiomers by chromatography,[9–17] sensing of chiral molecules,[18–21] and circularly polarized luminescence.[22–27] The application of optically active helical polymers for asymmetric catalysis has also attracted growing interest, because a one-handed helical chirality can significantly contribute to the enantioselectivity due to a one-handed helical arrangement of the catalytically active, chiral/achiral units along the one-handed helical polymer backbone.[8,28–30] Up to now, a variety of helical polymer-based asymmetric catalysts have been developed mainly by introducing catalytically active, chiral/achiral units as components in or along artificial helical polymers that involve polyacetylenes,[31–35] poly(methacrylate)s,[36–38] polyisocyanates,[37] polyisocyanides,[39–41] and poly(quinoxaline-2,3-diyl)s.[29,30,42–44] In these cases, the use of optically active monomers is essential to control their helical handedness except for poly(methacrylate)s with a bulky pendant prepared by helix-sense-selective polymerization using chiral catalysts or initiators.[2,5,45] Otherwise, racemic helices with no optical activity will be produced, thus showing no enantioselective catalytic activity.

We previously reported a conceptually new and versatile method, namely "helicity induction and memory" principle,[8,18,19,46–48] to develop helical polymer-based asymmetric catalysts. A preferred-handed helix induced in an optically inactive polyisocyanide via noncovalent chiral interactions with optically active guests is retained ("memorized") after complete removal of the optically active guests. Further modification of the pendant groups with catalytically active, but achiral units, produces functional helical polyisocyanides while maintaining the helicity memory, which catalyzes the asymmetric direct aldol reaction, although its

Additional supporting information may be found in the online version of this article.

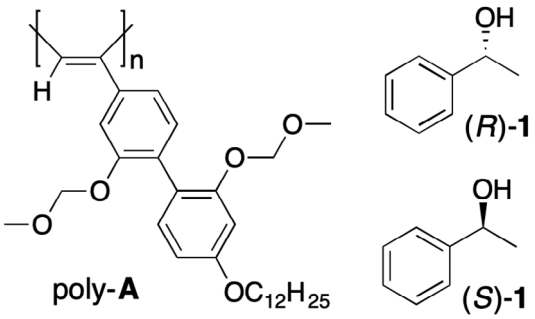

CHART 1 Structures of PBA (poly-**A**) and optically active alcohols ((*R*)-**1** and (*S*)-**1**).

enantioselectivity was rather low, providing the first polymer-based asymmetric catalysts based on the helicity memory.[39] This "helicity induction and memory" concept has recently been applied to dynamic helical poly(quinoxaline-2,3-diyl)s to develop powerful asymmetric catalysts by Nagata *et al.*[49]

Recently, we also found unique helical polymers, poly(biphenylylacetylene)s (PBAs), such as poly-**A** (Chart 1), to which the "helicity induction and memory" principle can be applied.[13,50] In fact, poly-**A** formed a preferred-handed helical conformation through noncovalent chiral interactions with the optically active 1-phenylethanol ((*R*)-**1** and (*S*)-**1**) both in solution and the solid state, and the macromolecular helicity induced in the PBA backbones could be memorized after complete removal of the optically active alcohols. Taking advantage of this helicity induction followed by memory of the helicity, we successfully developed the first smart chiral stationary phase (CSP) capable of switching the elution order of enantiomers. The observed reversible switching of the enantioseparation ability of poly-**A** relies on the switching of the macromolecular helicity by sequential column treatments with optically active compounds, such as (*R*)- and (*S*)-**1**. The successful application of poly-**A** to the switchable CSP implies that helical polymer-based switchable asymmetric catalysts could also be developed based on the unique helicity induction and memory effect observed for PBAs by introducing the catalytically active, achiral residues at the pendant groups of the PBAs.

To this end, we designed and synthesized novel PBAs (poly-**2a** and poly-**2b**) bearing pyridine *N*-oxide groups with a bulky (poly-**2a**) or a less-bulky substituent (poly-**2b**) at a different position as catalytically active units at the 4′-position of the biphenyl pendants and investigated their helicity induction and memory effects along with their asymmetric catalytic activities for the allylation of benzaldehydes with allyltrichlorosilane (Fig. 1).[51]

EXPERIMENTAL

The monomers (**2a** and **2b**) were synthesized according to Scheme 1(a,b).

Synthesis of 2-(*p*-Dodecyloxyphenyl)pyridine (5)

To a solution of 2-(*p*-dodecyloxyphenyl)-4,4,5,5-tetramethyl-1,3,2-dioxaborolane (7.28 g, 18.7 mmol), 2-bromopyridine (1.17 mL, 12.1 mmol), and potassium carbonate (4.58 g, 33.1 mmol) in a degassed 1,2-dimethoxyethane–water mixture (3/1, v/v; 316 mL) was added tetrakis(triphenylphosphine) palladium(0) (1.05 g, 0.909 mmol). The mixture was stirred at 80 °C for 5 h. After evaporating the solvent, the residue was diluted with an *n*-hexane–ethyl acetate mixture (10/1, v/v) and the solution was washed with water and brine, and then dried over $MgSO_4$. The solvent was removed under reduced pressure and the crude product was purified by silica gel chromatography using *n*-hexane–ethyl acetate (5/1, v/v) as the eluent to give the desired product as a yellow solid (3.48 g, 86% yield). ^{1}H NMR (500 MHz, $CDCl_3$, rt): δ 8.64–8.66 (m, 1H, Ar—H), 7.92–7.95 (m, 2H, Ar—H), 7.66–7.73 (m, 2H, Ar—H), 7.15–7.18 (m, 1H, Ar—H), 6.97–7.00 (m, 2H, Ar—H), 4.01 (t, J = 6.6 Hz, 2H, OCH_2CH_2), 1.81 (quint, J = 7.1 Hz, 2H, CH_2CH_2), 1.26–1.47 (m, 18H, CH_2), 0.88 (t, J = 6.5 Hz, 3H, CH_2CH_3). ^{13}C NMR (126 MHz, $CDCl_3$, rt): δ 160.07, 157.22, 149.53, 136.64, 131.79, 128.12, 121.34, 119.78, 114.69, 68.12, 31.93, 29.68, 29.65, 29.61, 29.59, 29.42, 29.36, 29.27, 26.06, 22.70, 14.13. HRMS (ESI+): m/z calcd for $C_{23}H_{34}NO$ ($M + H^+$), 340.2635; found 340.2695.

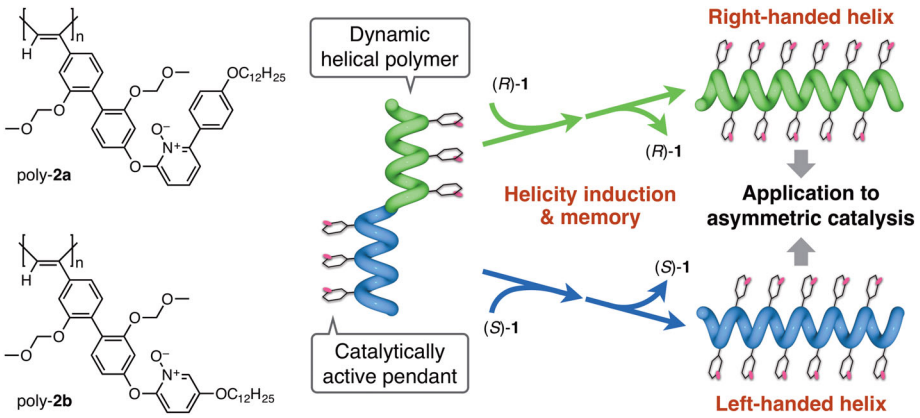

FIGURE 1 Structures of poly-**2a** and poly-**2b** and schematic illustration of the development of helical polymer-based asymmetric catalysts based on the helicity induction and its memory strategy. [Color figure can be viewed at wileyonlinelibrary.com]

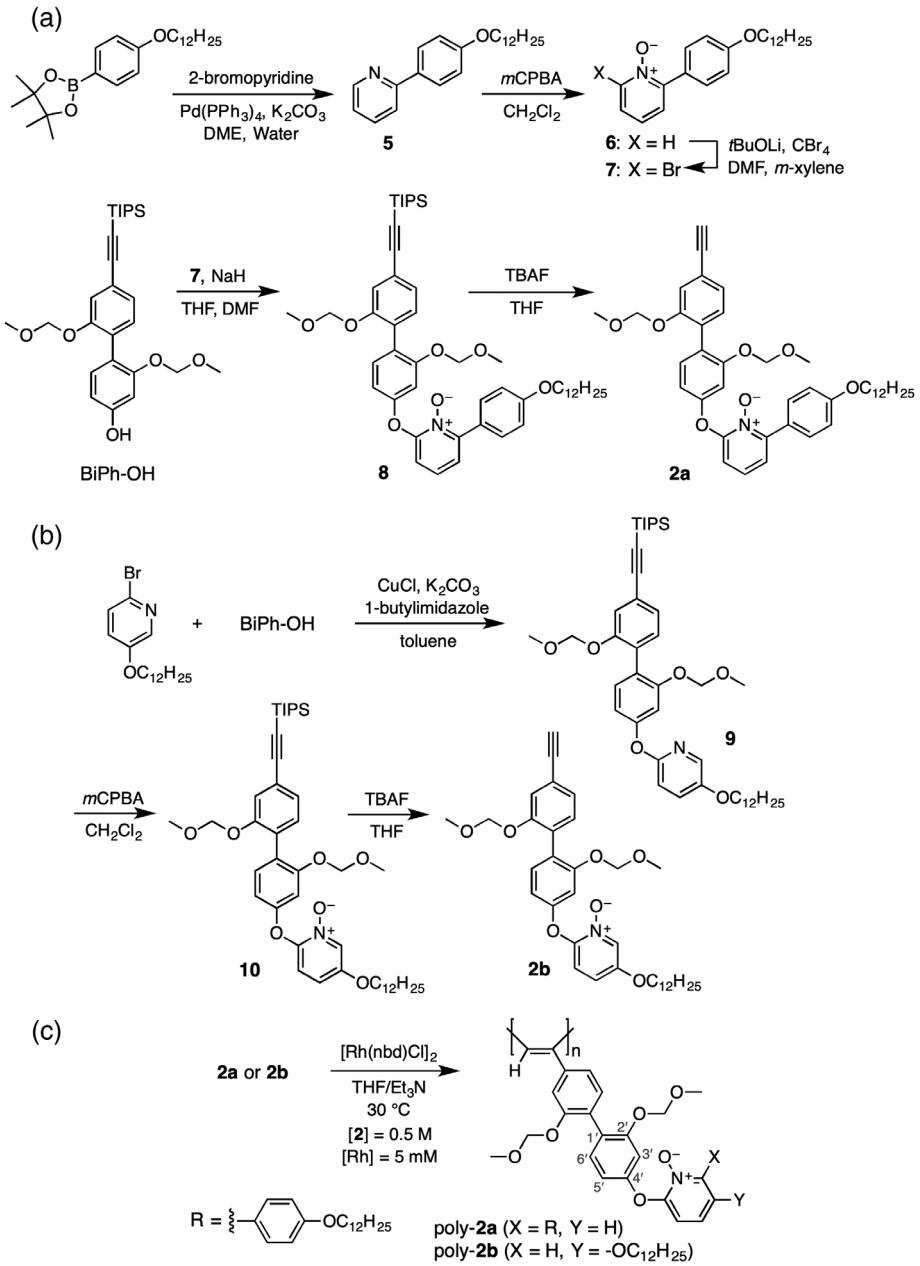

SCHEME 1 Syntheses of **2a** (a), **2b** (b), and poly-**2** (c).

Synthesis of 2-(*p*-Dodecyloxyphenyl)pyridine 1-Oxide (6) **5** (3.29 g, 9.96 mmol) was dissolved in anhydrous dichloromethane (97 mL) and the solution was cooled to 0 °C. To this was added 3-chloroperoxybenzoic acid (*m*CPBA) (3.59 g, 20.8 mmol) dissolved in anhydrous dichloromethane (36 mL), and the mixture was stirred at room temperature for 48 h. After evaporating the solvent, the residue was diluted with chloroform and the solution was washed with saturated $NaHCO_3$ aqueous solution and brine, and then dried over $MgSO_4$. The solvent was removed under reduced pressure and the crude product was purified by silica gel chromatography using chloroform–methanol (95/5, v/v) as the eluent to give the desired product as a yellow solid (3.01 g, 87% yield). IR (KBr, cm^{-1}): 1246 (N═O). ^{1}H NMR (500 MHz, $CDCl_3$, rt): δ 8.32 (d, J = 6.8 Hz, 1H, Ar—H), 7.80–7.83 (m, 2H, Ar—H), 7.42 (dd, J = 7.9, 2.1 Hz, 1H, Ar—H), 7.27–7.29 (m, 1H, Ar—H), 7.16–7.19 (m, 1H, Ar—H), 6.97–7.00 (m, 2H, Ar—H), 4.01 (t, J = 6.6 Hz, 2H, OCH_2CH_2), 1.80 (quint, J = 7.1 Hz, 2H, CH_2CH_2), 1.27–1.49 (m, 18H, CH_2), 0.88 (t, J = 7.0 Hz, 3H, CH_2CH_3). ^{13}C NMR (126 MHz, $CDCl_3$, rt): δ 160.21, 140.57, 130.77, 126.95, 125.69, 124.58, 123.82, 114.26, 68.13, 31.93, 29.67, 29.64, 29.61, 29.59, 29.39, 29.36, 29.19, 26.02, 22.70, 14.13. HRMS (ESI+): m/z calcd for $C_{23}H_{33}NNaO_2$ ($M + Na^+$), 378.2404; found 378.2457.

Synthesis of 2-Bromo-6-(*p*-dodecyloxyphenyl)pyridine 1-Oxide (7)

6 (3.12 g, 8.44 mmol), lithium *tert*-butoxide (2.70 g, 33.8 mmol), and carbon tetrabromide (6.99 g, 21.1 mmol) were dissolved in anhydrous *N*,*N*-dimethylformamide (DMF)–*m*-xylene (1/1, v/v; 8 mL) and the mixture was stirred at 40 °C for 1.5 h. After quenching the reaction with water, the mixture was diluted with ethyl acetate and the solution was washed with brine and then dried over $MgSO_4$. The solvent was removed under reduced pressure and the crude product was purified by silica gel chromatography using *n*-hexane–ethyl acetate (1/1, v/v) as the eluent to give the desired product as a light brown solid (1.20 g, 32% yield). IR (KBr, cm^{-1}): 1245 (N═O). ^{1}H NMR (500 MHz, $CDCl_3$, rt): δ 7.79–7.82 (m, 2H, Ar—H), 7.60 (dd, J = 7.9, 2.1 Hz, 1H, Ar—H), 7.38 (dd, J = 7.9, 2.1 Hz, 1H, Ar—H), 7.10 (t, J = 8.0 Hz 1H, Ar—H), 6.95–6.98 (m, 2H, Ar—H), 4.01 (t, J = 6.6 Hz, 2H, OCH_2CH_2), 1.80 (quint, J = 7.1 Hz, 2H, CH_2CH_2), 1.27–1.49 (m, 18H, CH_2), 0.88 (t, J = 7.1 Hz, 3H, CH_2CH_3). ^{13}C NMR (126 MHz, $CDCl_3$, rt): δ 160.41, 150.75, 134.56, 130.89, 128.77, 125.47, 124.89, 124.65, 114.11, 68.15, 31.92, 29.67, 29.64, 29.61, 29.58, 29.39, 29.36, 29.19, 26.02, 22.70, 14.13. HRMS (ESI+): m/z calcd for $C_{23}H_{32}BrNNaO_2$ (M + Na^+), 456.1509; found 456.1562.

Synthesis of 8

To a mixture of ((2,2′-bis(methoxymethoxy)-4′-hydroxy-4-biphenylyl)ethynyl)triisopropylsilane (BiPh-OH) (0.32 g, 0.69 mmol) and sodium hydride (60% dispersion in mineral oil; 49 mg, 1.0 mmol) in anhydrous DMF (3.0 mL) was added an anhydrous tetrahydrofuran (THF) solution (12.5 mL) of **7** (0.30 g, 0.69 mmol). The mixture was stirred at 100 °C for 4 h. After evaporating the solvent, the residue was diluted with ethyl acetate and the solution was washed with water and brine, and then dried over $MgSO_4$. The solvent was removed under reduced pressure and the crude product was purified by silica gel chromatography using *n*-hexane–ethyl acetate (1/2, v/v) as the eluent to give the desired product as a yellow oil (449 mg, 79% yield). IR (neat, cm^{-1}): 2150 (C≡C), 1250 (N═O). ^{1}H NMR (500 MHz, $CDCl_3$, rt): δ 7.87–7.90 (m, 2H, Ar—H), 7.29 (d, J = 1.4 Hz, 1H, Ar—H), 7.15–7.25 (m, 5H, Ar—H), 7.07 (d, J = 2.4 Hz, 1H, Ar—H), 6.96–7.00 (m, 3H, Ar—H), 6.69 (dd, J = 8.4, 2.5 Hz, 1H, Ar—H), 5.08 (s, 2H, OCH_2O), 5.04 (s, 2H, OCH_2O), 4.01 (t, J = 6.5 Hz, 2H, OCH_2CH_2), 3.36 (s, 3H, OCH_3), 3.33 (s, 3H, OCH_3), 1.80 (quint, J = 7.5 Hz, 2H, CH_2CH_2), 1.27–1.49 (m, 18H, CH_2), 1.14 (s, 21H, TIPS), 0.88 (t, J = 7.1 Hz, 3H, CH_2CH_3). ^{13}C NMR (126 MHz, $CDCl_3$, rt): δ 160.29, 156.89, 156.03, 155.16, 154.65, 150.34, 132.01, 131.44, 130.97, 128.94, 125.89, 125.54, 124.77, 124.47, 123.87, 121.28, 118.54, 114.13, 112.99, 110.70, 106.89, 106.17, 95.18, 95.15, 90.69, 68.14, 56.05, 55.99, 31.93, 29.67, 29.65, 29.61, 29.59, 29.39, 29.36, 29.20, 26.02, 22.70, 18.69, 14.13, 11.35. HRMS (ESI+): m/z calcd for $C_{50}H_{69}NNaO_7Si$ (M + Na^+), 846.4736; found 846.4730.

Synthesis of 2a

To a solution of **8** (400 mg, 0.49 mmol) in anhydrous THF (19 mL) was added tetra-*n*-butylammonium fluoride (TBAF) (1.0 M in THF, 0.58 mL, 0.58 mmol) at 0 °C and the mixture was stirred at 0 °C for 1 h. After evaporating the solvent, the residue was diluted with ethyl acetate and the solution was washed with water and brine, and then dried over $MgSO_4$. The solvent was removed under reduced pressure and the residual compound was passed through a short pad of silica gel using chloroform–methanol (97/3, v/v) as the eluent. After concentrating in vacuo, the crude product was purified by recycling preparative high-performance liquid chromatography (HPLC) on JAIGEL-1H and JAIGEL-2H (60 cm × 2.0 cm [i.d.]) to give the desired product as colorless oil (247 mg, 75% yield). IR (KBr, cm^{-1}): 3284 (≡CH), 2106 (C≡C), 1250 (N═O). ^{1}H NMR (500 MHz, $CDCl_3$, rt): δ 7.87–7.90 (m, 2H, Ar—H), 7.35 (d, J = 1.5 Hz, 1H, Ar—H), 7.17–7.26 (m, 5H, Ar—H), 7.06 (d, J = 2.4 Hz, 1H, Ar—H), 7.01 (dd, J = 7.4, 2.6 Hz, 1H, Ar—H), 6.97–6.99 (m, 2H, Ar—H), 6.69 (dd, J = 8.2, 2.4 Hz, 1H, Ar—H), 5.07 (s, 2H, OCH_2O), 5.04 (s, 2H, OCH_2O), 4.01 (t, J = 6.6 Hz, 2H, OCH_2CH_2), 3.36 (s, 3H, OCH_3), 3.33 (s, 3H, OCH_3), 3.08 (s, 1H, C≡C—H), 1.80 (quint, J = 7.5 Hz, 2H, CH_2CH_2), 1.27–1.49 (m, 18H, CH_2), 0.88 (t, J = 7.1 Hz, 3H, CH_2CH_3). ^{13}C NMR (126 MHz, $CDCl_3$, rt): δ 160.28, 156.75, 156.01, 155.27, 154.74, 150.33, 131.96, 131.55, 130.97, 129.36, 125. 65, 125.55, 124.54, 124.43, 122.33, 121.37, 118.91, 114.12, 113.17, 110.60, 106.12, 95.21, 95.16, 83.52, 68.12, 56.01, 55.99, 31.92, 29.67, 29.64 29.61, 29.58, 29.39, 29.36, 29.18, 26.01, 22.70, 14.14. HRMS (ESI+): m/z calcd for $C_{41}H_{49}NNaO_7$ (M + Na^+), 690.3401; found 690.3435.

Synthesis of 9

To a mixture of BiPh-OH (496 mg, 1.06 mmol), 2-bromo-5-dodecyloxypyridine (365 mg, 1.06 mmol), copper(I) chloride (11.6 mg, 0.117 mmol), and potassium carbonate (292 mg, 2.11 mmol) in anhydrous toluene (2.2 mL) was added 1-butylimidazole (69 μL, 0.53 mmol). The mixture was stirred at 120 °C for 16 h. After evaporating the solvent, the residue was diluted with ethyl acetate and the solution was washed with water and brine, and then dried over $MgSO_4$. The solvent was removed under reduced pressure and the crude product was purified by silica gel chromatography using *n*-hexane–ethyl acetate (8/1, v/v) as the eluent to give the desired product as a yellow solid (662 mg, 86% yield). IR (KBr, cm^{-1}): 2156 (C≡C). ^{1}H NMR (500 MHz, $CDCl_3$, rt): δ 7.91 (d, J = 3.3 Hz, 1H, Ar—H), 7.27–7.30 (m, 2H, Ar—H), 7.17–7.19 (m, 3H, Ar—H), 6,99 (d, J = 2.5 Hz, 1H, Ar—H), 6.91 (d, J = 8.8 Hz, 1H, Ar—H), 6.75 (dd, J = 8.3, 2.1 Hz, 1H, Ar—H), 5.08 (s, 2H, OCH_2O), 5.04 (s, 2H, OCH_2O), 3.97 (t, J = 6.6 Hz, 2H, OCH_2CH_2), 3.36 (s, 3H, OCH_3), 3.33 (s, 3H, OCH_3), 1.78 (quint, J = 7.1 Hz, 2H, CH_2CH_2), 1.27–1.48 (m, 18H, CH_2), 0.88 (t, J = 7.0 Hz, 3H, CH_2CH_3). ^{13}C NMR (126 MHz, $CDCl_3$, rt): δ 157.06, 155.87, 155.74, 154.70, 152.12, 133.66, 131.72, 131.54, 129.36, 126.74, 125.89, 123.86, 123.66, 118.59, 112.87, 112.72, 107.61, 106.99, 95.21, 95.09, 90.53, 69.14, 56.03, 55.95, 31.92, 29.66, 29.64, 29.60, 29.57, 29.37, 29.35, 29.26, 25.96, 22.70, 18.17, 14.12, 11.35. HRMS (ESI+): m/z calcd for $C_{44}H_{65}NNaO_6Si$ (M + Na^+), 754.4473; found 754.4483.

Synthesis of 10

9 (631 mg, 0.861 mmol) was dissolved in anhydrous dichloromethane (8.9 mL) and the solution was cooled to 0 °C. To this was added *m*CPBA (297 mg, 1.72 mmol) dissolved in

anhydrous dichloromethane (2.0 mL), and the mixture was stirred at room temperature for 48 h. After evaporating the solvent, the residue was diluted with chloroform and the solution was washed with saturated $NaHCO_3$ aqueous solution and brine, and then dried over $MgSO_4$. The solvent was removed under reduced pressure and the crude product was purified by silica gel chromatography using chloroform–methanol (94/6, v/v) as the eluent to give the desired product as a yellow oil (384 mg, 59% yield). IR (neat, cm^{-1}): 2150 (C≡C), 1244 (N═O). ^1H NMR (500 MHz, $CDCl_3$, rt): δ 8.05 (d, J = 2.5 Hz, 1H, Ar—H), 7.28 (d, J = 1.5 Hz, 1H, Ar—H), 7.14–7.20 (m, 3H, Ar—H), 6.99–7.01 (m, 2H, Ar—H), 6.89 (dd, J = 9.1, 2.6 Hz, 1H, Ar—H), 6.58 (dd, J = 8.4, 2.5 Hz, 1H, Ar—H), 5.07 (s, 2H, OCH_2O), 5.04 (s, 2H, OCH_2O), 3.95 (t, J = 6.5 Hz, 2H, OCH_2CH_2), 3.35 (s, 3H, OCH_3), 3.33 (s, 3H, OCH_3), 1.79 (quint, J = 7.0 Hz, 2H, CH_2CH_2), 1.27–1.47 (m, 18H, CH_2), 1.14 (s, 21H, TIPS), 0.88 (t, J = 7.0 Hz, 3H, CH_2CH_3). ^{13}C NMR (126 MHz, $CDCl_3$, rt): δ 157.02, 155.68, 154.64, 153.29, 150.36, 131.94, 131.42, 128.93 128.04, 125.89, 124.52, 123.86, 118.56, 115.90, 115.81, 109.77, 106.89, 105.57, 95.18, 95.11, 90.69, 69.57, 56.05, 56.00, 31.92, 29.65, 29.63, 29.57, 29.52, 29.35, 29.28, 28.93, 25.85, 22.69, 18.17, 14.12, 11.34. HRMS (ESI+): m/z calcd for $C_{44}H_{65}NNaO_7Si$ ($M + Na^+$), 770.4423; found 770.4428.

Synthesis of 2b

To a solution of **10** (350 mg, 0.47 mmol) in anhydrous THF (19 mL) was added TBAF (1.0 M in THF, 0.56 mL, 0.56 mmol) at 0 °C and the mixture was stirred at 0 °C for 1 h. After evaporating the solvent, the residue was diluted with ethyl acetate and the solution was washed with water and brine, and then dried over $MgSO_4$. The solvent was removed under reduced pressure and the residual compound was passed through a short pad of silica gel using chloroform–methanol (96/4, v/v) as the eluent. After concentrating in vacuo, the crude product was purified by recycling preparative HPLC on JAIGEL-1H and JAIGEL-2H (60 cm × 2.0 cm [i.d.]) to give the desired product as a white solid (149 mg, 54% yield). Mp: 73.2–74.0 °C. IR (KBr, cm^{-1}): 3259 (≡CH), 2103 (C≡C), 1240 (N═O). ^1H NMR (500 MHz, $CDCl_3$, rt): δ 8.05 (d, J = 2.7 Hz, 1H, Ar—H), 7.34 (d, J = 1.2 Hz, 1H, Ar—H), 7.15–7.20 (m, 3H, Ar—H), 7.00–7.02 (m, 2H, Ar—H), 6.89 (dd, J = 9.2, 2.7 Hz, 1H, Ar—H), 6.58 (dd, J = 8.2, 2.4 Hz, 1H, Ar—H), 5.06 (s, 2H, OCH_2O), 5.04 (s, 2H, OCH_2O), 3.96 (t, J = 6.6 Hz, 2H, OCH_2CH_2), 3.35 (s, 3H, OCH_3), 3.33 (s, 3H, OCH_3), 3.08 (s, 1H, C≡C—H), 1.82 (quint, J = 7.0 Hz, 2H, CH_2CH_2), 1.27–1.47 (m, 18H, CH_2), 0.88 (t, J = 7.0 Hz, 3H, CH_2CH_3).^{13}C NMR (126 MHz, $CDCl_3$, rt): δ 155.98, 155.77, 154.71, 153.32, 150.24, 131.88, 131.51, 129.34, 128.03, 125.64, 124.29, 122.32, 118.93, 116.02, 115.73, 109.67, 105.54, 95.19, 95.17, 83.50, 69.55, 56.00, 31.91, 29.64, 29.63, 29.57, 29.52, 29.35, 29.27, 28.92, 25.83, 22.69, 14.12. HRMS (ESI+): m/z calcd for $C_{35}H_{45}NNaO_7$ ($M + Na^+$), 614.3088; found 614.3103.

Polymerization

The polymerizations of **2a** and **2b** were carried out according to Scheme 1(c) in a dry glass ampule under a dry nitrogen atmosphere using [(norbornadiene)rhodium(I) chloride]$_2$ ([Rh(nbd)Cl]$_2$) as a catalyst in a similar way as previously reported.[13,50]

A typical procedure for the polymerization of **2a** is described as follows. The monomer **2a** (100 mg, 0.15 mmol) was placed in a dry ampule, which was then evacuated on a vacuum line and flushed with dry nitrogen. After this evacuation-flush procedure was repeated three times, a three-way stopcock was attached to the ampule, and freshly distilled THF (0.25 mL) and triethylamine (Et_3N) (63 μL, 0.45 mmol) were added using a syringe. To this was added a solution of [Rh(nbd)Cl]$_2$ (0.03 M) in distilled THF (50 μL) at 30 °C. The concentrations of the monomer and the rhodium catalyst were 0.5 and 0.005 M, respectively. After 3 h, THF (2 mL) was added to the reaction mixture. The resulting polymer was then precipitated into a large amount of methanol and collected by centrifugation. The obtained poly-**2a** was washed with methanol and dried in vacuo (91 mg, 91% yield). In the same way, poly-**2b** was prepared. The M_n and M_w/M_n of the polymers were determined by size-exclusion chromatography (SEC) using polystyrene standards in THF. The polymerization results are summarized in Supporting Information Table S1.

Spectroscopic data of poly-**2a**: IR (KBr, cm^{-1}) 1251 (N═O). ^1H NMR (500 MHz, $CDCl_3$, 50 °C): δ 7.88–7.80 (br, 2H, Ar—H), 7.20–7.00 (br, 2H, Ar—H), 7.00–6.70 (br, 7H, Ar—H), 6.50–6.35 (br, 2H, Ar—H), 6.05–5.85 (br, 1H, C═CH), 4.85–4.60 (br, 4H, $2OCH_2O$), 3.98–3.85 (br, 2H, OCH_2CH_2), 3.13–2.86 (br, 6H, $2OCH_3$), 1.80–1.72 (br, 2H, OCH_2CH_2), 1.46–1.20 (br, 18H, CH_2), 0.87 (br, 3H, CH_3). Calcd for $C_{41}H_{49}NO_7$: C, 73.74; H, 7.40; N, 2.10. Found: C, 73.75; H, 7.25; N, 2.06.

Spectroscopic data of poly-**2b**: IR (KBr, cm^{-1}) 1241 (N═O). ^1H NMR (500 MHz, $CDCl_3$, 50 °C): δ 7.98–7.94 (br, 1H, Ar—H), 6.92–6.76 (br, 6H, Ar—H), 6.50–6.35 (br, 2H, Ar—H), 6.05–5.85 (br, 1H, C═CH), 4.85–4.60 (br, 4H, $2OCH_2O$), 3.98–3.85 (br, 2H, OCH_2CH_2), 3.13–2.86 (br, 6H, $2OCH_3$), 1.80–1.72 (br, 2H, OCH_2CH_2), 1.46–1.20 (br, 18H, CH_2), 0.87 (br, 3H, CH_3). Calcd for $C_{35}H_{45}NO_7$: C, 71.04; H, 7.67; N, 2.37. Found: C, 71.03; H, 7.77; N, 2.34.

Typical Procedure for Asymmetric Allylation of Benzaldehyde with Allyltrichlorosilane

$hm_{(R)5}$-Poly-**2b** (3 μmol based on the pyridine *N*-oxide residue of poly-**2b**) was dissolved in toluene (0.16 mL) under an argon atmosphere. To this was added **3a** (3.6 mg, 0.034 mmol) dissolved in toluene (20 μL), *N*-ethyldiisopropylamine ($^iPr_2NEt$) (18 μL, 0.10 mmol), and allyltrichlorosilane (8.9 mg, 0.051 mmol) dissolved in toluene (30 μL) at −10 °C. The mixture was stirred at −10 °C for 6 h. After the addition of aqueous NaOH (1.0 M, 0.20 mL) to quench the reaction, chloroform was added, and the organic layer was washed with brine and dried over anhydrous $MgSO_4$. After filtration, the solvent was evaporated to dryness in vacuo. The conversion of **3a** to the allyl alcohol **4a** was determined to be 21% by ^1H NMR analysis using 1,1,2,2-tetrachloroethane as the internal standard. After the residue was passed through a short pad of silica gel using chloroform as the eluent, the enantiomeric excess (ee) value of the product **4a** (5% ee, *S*-rich) was determined by chiral HPLC

analysis using a CHIRALCEL OD-H column (*n*-hexane–2-propanol (98/2, v/v); flow rate 0.8 mL/min; temperature about 20 °C: t_r = 18.5 min (for *R*-isomer), t_r = 21.0 min (for *S*-isomer) (see Supporting Information Fig. S9).[52] Allylation reactions of **3b** and **3c** with allyltrichlorosilane were also performed in a similar manner and the results are summarized in Table 1.

Chromatographic condition for the ee determination of **4b**: CHIRALCEL OD-H column (*n*-hexane–2-propanol (98/2, v/v); flow rate 0.8 mL/min; temperature about 20 °C: t_r = 26.0 min (for *R*-isomer), t_r = 31.7 min (for *S*-isomer).[52]

Chromatographic condition for the ee determination of **4c**: CHIRALCEL OB-H column (*n*-hexane–2-propanol (90/10, v/v); flow rate 0.8 mL/min; temperature about 20 °C: t_r = 16.4 min (for *S*-isomer), t_r = 17.8 min (for *R*-isomer).[52]

RESULTS AND DISCUSSION

Synthesis

The synthetic route to prepare novel biphenylylacetylene monomers (**2a** and **2b**) containing pyridine *N*-oxide groups as a catalytically active pendant is shown in Scheme 1(a,b), respectively. The molecular design of **2a** with a bulky *p*-alkoxyphenyl substituent at the *o*-position of the pyridine *N*-oxide group was based on the previously reported pyridine *N*-oxide-based asymmetric catalysts developed by Hayashi *et al*.[53] The target monomer **2a** was synthesized from a previously reported 4-phenylphenol derivative (BiPh-OH)[54] through etherification with 2-bromo-6-(*p*-dodecyloxyphenyl)pyridine 1-oxide followed by deprotection of a triisopropylsilyl group. The analogous monomer **2b** with a long alkoxy substituent at the *m*-position of the pyridine *N*-oxide group was also prepared from BiPh-OH in a similar manner. The rhodium-catalyzed polymerization of the obtained **2a** and **2b** was performed in a THF/Et_3N mixture at 30 °C according to a previously reported procedure (Scheme 1(c) and Supporting Information Table S1).[13,50] Optically inactive PBAs, poly-**2a** and poly-**2b**, carrying different pyridine *N*-oxide pendants were obtained in good yields (≥82%) with the number-average molecular weight (M_n) of 4.2×10^5 and 2.1×10^5, respectively, as estimated by SEC. ^{1}H NMR analysis revealed that the stereoregularities of the obtained polymers were almost completely *cis-transoidal* (Supporting Information Fig. S1).

Helicity Induction and Static Memory

The preferred-handed helicity induction ability of the optically inactive poly-**2a** was first investigated using (*R*)-**1** and (*S*)-**1** as helix inducers in toluene (**1**/toluene, 5:95, v/v) at 25 °C. Poly-**2a** showed an induced circular dichroism (ICD) in the absorption region of the polyacetylene backbone and its intensity increased with time and became constant within 1 h [Fig. 2(a) and Supporting Information Fig. S2]. Although the saturated ICD intensity of poly-**2a** in (*R*)-**1**/toluene (5/95, v/v) tended to decrease with the increasing temperature, an excess handed helix was induced in poly-**2a** to some extent even at 50 °C (Supporting Information Fig. S3). As expected, poly-**2a** exhibited a perfect mirror-image CD spectrum when the antipode (*S*)-**1** was used instead of (*R*)-**1** [Fig. 2(a)(ix)]. These results indicated that the poly-**2a** formed a preferred-handed helical conformation in response to the chirality of optically active guests. Based on the relationships between the Cotton effect signs and the helical handedness of analogous helical poly(phenylacetylene)s,[55–58] the poly-**2a** backbone most likely had left- and right-handed helical conformations in toluene containing (*R*)-**1** and (*S*)-**1** (5 vol%), respectively. The CD spectral pattern of poly-**2a** was similar to that of the previously reported poly-**A** with a one-handed macromolecular helicity,[13] indicating that the pyridine *N*-oxide-based functional group introduced at the 4′-position of the biphenyl pendant caused a negligible structural alteration in the helical polyacetylene backbone.

We found that the main-chain absorption band of poly-**2a** in (*R*)-**1**/toluene mixtures at 25 °C was significantly red-shifted as the volume fraction of (*R*)-**1** increased, resulting in the absorbance maximum (ε_{max}) at 458 nm in (*R*)-**1**/toluene (40/60 and 50/50, v/v) [Fig. 2(a)(vii, viii)] accompanied by a color change from yellow to orange. Similar absorption spectral changes were also observed when *rac*-**1** was used instead of (*R*)-**1** (Supporting Information Fig. S4). Therefore, the observed red-shift of the absorption spectra of poly-**2a** with the color changes can be ascribed to a solvent-induced main-chain conformational change from a tightly twisted helix to an extended helix, leading to elongation of the π-conjugation length of the poly-**2a** backbone,[59] as observed in chloroform and dichloromethane (Supporting Information Fig. S5).

The ICD signals almost completely disappeared in toluene containing more than 30% (v/v) (*R*)-**1**, suggesting that poly-**2a** with an elongated π-conjugated backbone may not adopt a preferred-handed helical conformation [Fig. 2(a)(vi–viii)]. Interestingly, when (*R*)-**1**/toluene solutions (30/70 and 40/60, v/v) of poly-**2a** were cooled to −10 °C, the ICD signals appeared again along with a blue-shift of the absorption spectra and a recovery of the solution color from orange to yellow accompanied by inversion of the Cotton effect signs, while the absolute ICD intensities were almost comparable with those at 25 °C in (*R*)-**1**/toluene (5/95, v/v) [Fig. 2(b,c)]. Furthermore, both the absorption and CD spectra of poly-**2a** in (*R*)-**1**/toluene (30/70 and 40/60, v/v) at −10 °C were almost identical to those in (*S*)-**1**/toluene (5/95, v/v) at −10 °C. These results clearly revealed that both the right- and left-handed helices of poly-**2a** could be produced and completely switched using a single enantiomer by a change in temperature. Because poly-**2a** showed no concentration-dependent CD spectral changes (0.1–1.0 mM) and (Supporting Information Fig. S6), the formation of aggregates through intermolecular interactions could be excluded for the observed helix inversion. Interestingly, a one-handed helical conformation induced in the poly-**2b** backbone in (*R*)-**1**/toluene mixtures (1/99–40/60, v/v) at 25 as well as at −10 °C [Fig. 3(a,b)] was opposite (right-handed) to that of the poly-**2a** (left-handed) induced in (*R*)-**1**/toluene mixtures (1/99–20/80, v/v) at 25 °C. In addition, a unique temperature-driven helix-inversion observed in poly-**2a** did not take place for poly-**2b** in (*R*)-**1**/toluene (1/99–40/60, v/v) [Fig. 3(b)]. This may be ascribed to the

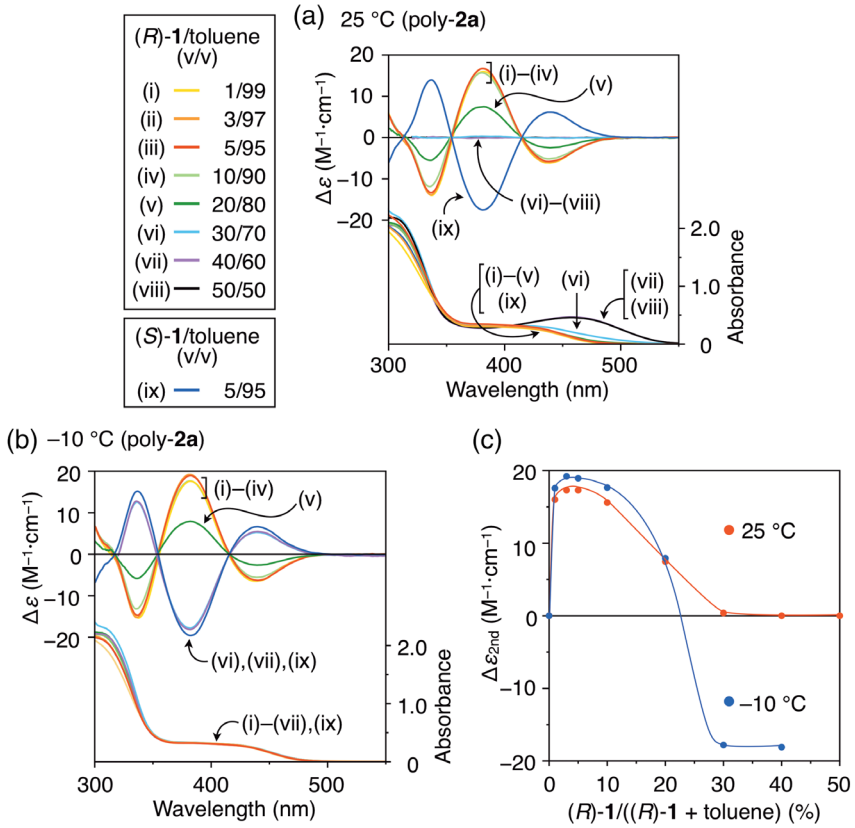

FIGURE 2 (a,b) CD and absorption spectra of poly-**2a** in (*R*)-**1**/toluene (1/99–50/50, v/v) or (*S*)-**1**/toluene (5/95, v/v) at 25 (a) and −10 °C (b). (c) Plots of ICD intensity ($\Delta\varepsilon_{2nd}$) of poly-**2a** measured at 25 (red circles) and −10 °C (blue circles) versus the volume fraction of (*R*)-**1** in a (*R*)-**1**/toluene mixture after standing at 25 and −10 °C, respectively, until no further increase in the ICD intensity was observed. [poly-**2a**] = 1.0 mM. [Color figure can be viewed at wileyonlinelibrary.com]

steric effect of the bulky (poly-**2a**) and less-bulky (poly-**2b**) substituents at different positions on the pyridine *N*-oxide groups.

The right- and left-handed helical poly-**2a** and poly-**2b** induced in toluene containing (*R*)-**1** or (*S*)-**1** (**1**/toluene = 5/95, v/v) at −10 °C [Fig. 4(a)(i,iii) and (b)(i,ii), respectively] were then isolated by precipitation into methanol to completely remove the optically active alcohols (Supporting Information Fig. S7). The CD spectral patterns and intensities of the isolated poly-**2a** [Fig. 4(a)(iv,vi)] and poly-**2b** [Fig. 4(b)(iii,iv)] in toluene at −10 °C were almost identical to those in the presence of the optically active (*R*)-**1** or (*S*)-**1** (5%, v/v). These results indicated that the induced right- and left-handed helices of poly-**2a** and poly-**2b** were almost completely memorized showing the complete mirror image CDs [Fig. 4(a,b)] as previously reported for poly-**A**.[14] Taking advantage of the unique helix-inversion of poly-**2a** in toluene with a different amounts of (*R*)-**1** (5/95 and 35/65, v/v) at −10 °C followed by static memory of the induced helices, the enantiomeric helices of poly-**2a** were also successfully memorized using a single enantiomer as a helix inducer [Fig. 4(a)(iv,v)]. Maeda *et al*. reported that a pair of enantiomeric helical polymers with a static helicity memory could be prepared from an achiral PBA by using a single enantiomeric helix inducer with the assistance of a temperature-driven helix inversion, although the helicity control was imperfect.[60] To the best of our knowledge, this is the first example of the preparation of both enantiomeric left- and right-handed helicity-memorized polymers with an almost perfect helical handedness using the chirality of a single enantiomer.[61]

The stabilities of the static helicity memories of poly-**2a** and poly-**2b** highly depended on the solvents and temperature (Supporting Information Fig. S8). For example, the isolated poly-**2a** and poly-**2b** from their (*R*)-**1**/toluene (5/95, v/v) solutions almost maintained their helicity memories in toluene at −10 °C for 24 h, while the CD intensities gradually decreased with time in toluene at 25 °C. In dichloromethane, however, the CD instantly disappeared at −10 °C (Supporting Information Fig. S8c).

Enantioselective Allylation Catalyzed by Pyridine *N*-Oxide-Appended Poly-2a and Poly-2b with a Static Helicity Memory

The optically active helical poly-**2a** and poly-**2b** with a static helicity memory were then utilized as organocatalysts for the enantioselective allylation of benzaldehydes (**3**) with allyltrichlorosilane in toluene at −10 °C (Scheme 2) to suppress the loss of helicity memory during the reactions (Supporting Information Fig. S8). The results are summarized in Table 1.

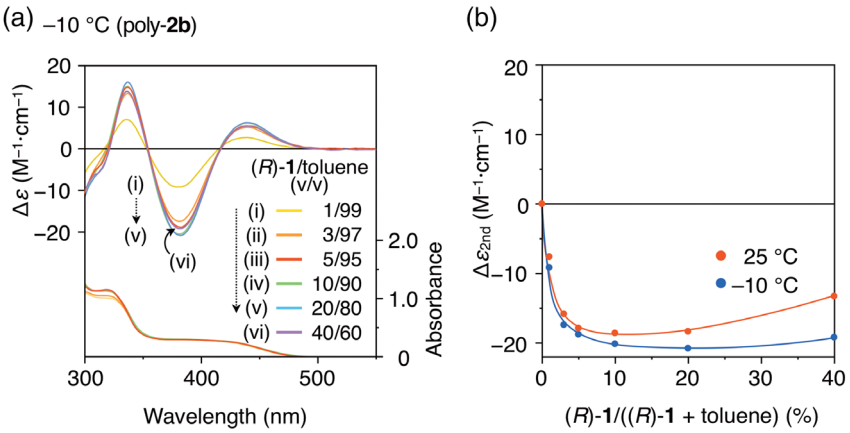

FIGURE 3 (a) CD and absorption spectra of poly-**2b** in (*R*)-**1**/toluene (1/99–40/60, v/v) at −10°C. (b) Plots of ICD intensity ($\Delta\varepsilon_{2nd}$) of poly-**2b** measured at 25 (red circles) and − 10°C (blue circles) versus the volume fraction of (*R*)-**1** in a (*R*)-**1**/toluene mixture after standing at 25 and −10°C, respectively, until no further increase in the ICD intensity was observed. [poly-**2b**] = 1.0 mM. [Color figure can be viewed at wileyonlinelibrary.com]

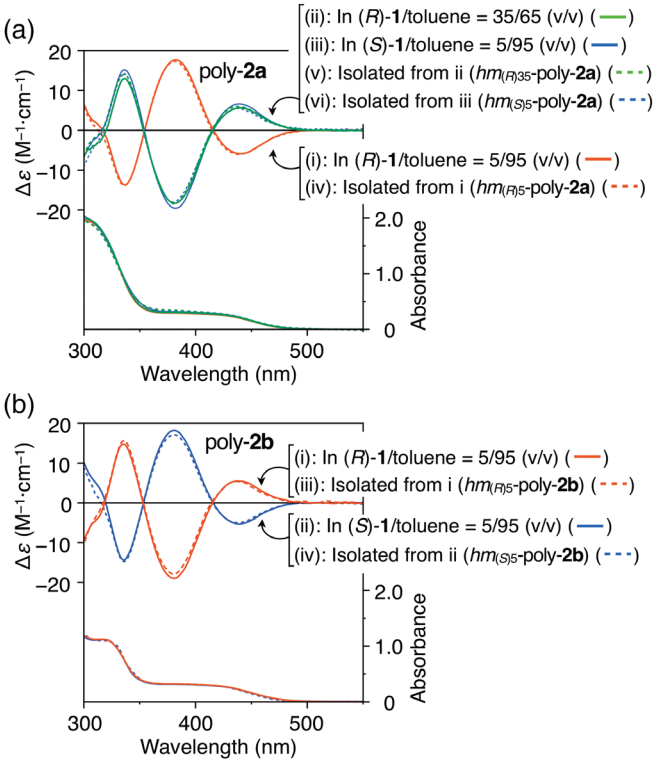

FIGURE 4 (a) CD and absorption spectra of poly-**2a** in the presence of (*R*)-**1** ((*R*)-**1**/toluene = 5/95 (i) and 35/65 (ii), v/v) or (*S*)-**1** ((*S*)-**1**/toluene = 5/95, v/v) (iii) after standing at −10°C until no further increase in the ICD intensity was observed, and those of the isolated poly-**2a** in toluene at −10°C recovered from (i) (iv; $hm_{(R)5}$-poly-**2a**), (ii) (v; $hm_{(R)35}$-poly-**2a**), and (iii) (vi; $hm_{(S)5}$-poly-**2a**), measured at −10°C. [poly-**2a**] = 1.0 mM. (b) CD and absorption spectra of poly-**2b** in the presence of (*R*)-**1** (i) or (*S*)-**1** (ii) (**1**/toluene = 5/95, v/v) after standing at −10°C until no further increase in the ICD intensity was observed and those of the isolated poly-**2b** in toluene at −10°C recovered from (i) (iii; $hm_{(R)5}$-poly-**2b**) and (ii) (iv; $hm_{(S)5}$-poly-**2b**), measured at −10°C. [poly-**2b**] = 1.0 mM. [Color figure can be viewed at wileyonlinelibrary.com]

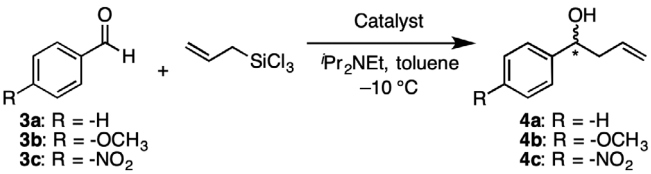

SCHEME 2 Allylation reactions of benzaldehydes (**3**) with allyltrichlorosilane catalyzed by achiral **2** and optically active and inactive poly-**2**.

Toluene was used instead of dichloromethane, a typical solvent for the asymmetric allylation reactions catalyzed by chiral pyridine *N*-oxide-based organocatalysts,[51–53,62–64] based on the stabilities of the helicity-memorized poly-**2a** and poly-**2b** (Supporting Information Fig. S8).

The as-prepared, optically inactive poly-**2a** and monomer **2a** as well as the helicity-memorized poly-**2a** ($hm_{(R)5}$-poly-**2a**) showed almost no catalytic activity in the allylation reaction of **3a** with allyltrichlorosilane (entries 1–3) mostly due to the steric and electronic environments around the catalytically active pyridine *N*-oxide residues of poly-**2a** and **2a**. In contrast, the as-prepared poly-**2b**, monomer **2b**, and the helicity-memorized poly-**2b** ($hm_{(R)5}$-poly-**2b**) bearing a less-bulky substituent around the catalytically active pyridine *N*-oxide sites catalyzed the allylation reaction of **3a** to produce the corresponding allyl alcohol (**4a**) (entries 4–6). Importantly, $hm_{(R)5}$-poly-**2b** could function as an asymmetric organocatalyst during the allylation reaction of **3a** with allyltrichlorosilane to produce **4a** with an optical activity, indicating the indispensable role of the macromolecular helicity memory of $hm_{(R)5}$-poly-**2b**, although its enantioselectivity (5% ee) was low (entry 6).

The enantioselectivity and catalytic activity of $hm_{(R)5}$-poly-**2b** toward the asymmetric allylation reaction were further investigated using *para*-methoxy (**3b**) and -nitro (**3c**) substituted benzaldehydes. Both the enantioselectivity and catalytic activity of $hm_{(R)5}$-poly-**2b** were significantly decreased for **4b**

TABLE 1 Enantioselective Allylation of Benzaldehydes (**3**) with Allyltrichlorosilane[a]

Entry	Catalyst	Substrate	Product	Time (h)	Conv. (%)[b]	ee (%)[c]
1	**2a**	**3a**	**4a**	24	<1	–
2	poly-**2a**	**3a**	**4a**	24	<1	–
3	*hm*$_{(R)5}$-poly-**2a**	**3a**	**4a**	24	<1	–
4	**2b**	**3a**	**4a**	6	11	–
5	poly-**2b**	**3a**	**4a**	6	20	–
6	*hm*$_{(R)5}$-poly-**2b**	**3a**	**4a**	6	21	5 (*S*)
7	*hm*$_{(R)5}$-poly-**2b**	**3b**	**4b**	6	10	<1
8	*hm*$_{(R)5}$-poly-**2b**	**3c**	**4c**	6	39	9 (*R*)
9	*hm*$_{(S)5}$-poly-**2b**	**3c**	**4c**	6	44	8 (*S*)

[a] The reactions of **3** (0.15 M) with allyltrichlorosilane (1.5 equiv) were carried out in the presence of a catalyst (10 mol %) and $^{i}Pr_2NEt$ (3.0 equiv.) in toluene at −10 °C.
[b] Determined by ^{1}H NMR analysis.
[c] Determined by chiral HPLC (see Supporting Information Fig. S9). In parentheses are shown the absolute configuration of the major enantiomer assigned by the retention times reported in the literature (Ref. 52).

(entry 7), but were only slightly improved for **4c** (39% conversion and 9% ee (*R*-rich)) (entry 8). The reason for this inversion of the enantioselectivity of *hm*$_{(R)5}$-poly-**2b** depending on the substrates (**3a** and **3c**) (entries 6 and 8 in Table 1) is not clear at present, but may be due to the electron-withdrawing nitro-substituent of **3c**. A similar inversion of the enantioselectivity depending on the substrates was reported by Kotora *et al*.[65] The fact that *hm*$_{(S)5}$-poly-**2b** with an opposite-handed helicity memory produced the product with the opposite configuration (8% ee (*S*-rich)) while maintaining its catalytic activity (entry 9) demonstrated that optically active helical polymers bearing achiral, but catalytically active residues as the pendants whose optical activities are solely derived from their static helicity memory indeed work as asymmetric catalysts, leading to the development of switchable asymmetric catalysts.

Apparently, the observed enantioselectivity of the helicity-memorized poly-**2b** in the allylation reactions evaluated in this study was unexpectedly low, mostly like because the catalytically active *N*-oxide units are located far from the helical polyacetylene backbone as well as the lack of stability of the helicity memory of the poly-**2b** during the allylation reactions even in toluene at −10 °C. The latter was evidenced by the fact that the CD intensity of the *hm*$_{(R)5}$-poly-**2b** significantly decreased by approximately one-fourth after the allylation reaction (Supporting Information Fig. S10), which was beyond our expectation [Supporting Information Fig. S8(a,b)] probably caused by some sort of reagents and/or products.

CONCLUSIONS

In summary, we have synthesized two novel PBA derivatives containing different types of pyridine *N*-oxide units as catalytically active achiral pendants. Each pair of enantiomeric helices with the static memory of the helicity was successfully produced through the noncovalent chiral interactions with a pair of enantiomeric alcohols or a single enantiomeric alcohol using temperature-driven inversion of the helicity, followed by complete removal of the chiral alcohols. A pair of enantiomeric helical PBA derivatives with the static helicity memory was found to catalyze the asymmetric allylation of benzaldehydes to produce optically active enantiomeric allyl alcohols. We believe that more powerful helical polymer-based asymmetric catalysts with a more stable one-handed helicity memory, showing a higher catalytic activity and switchable enantioselectivity based on a switchable memory of the helicity concept,[13] can be developed through the rational design of catalytically active pendants of helical PBAs with a unique static helicity memory. Further studies toward these goals are currently in progress in our laboratory and will be reported in due course.

ACKNOWLEDGMENTS

This work was supported by JSPS KAKENHI (Grant-in-Aid for Specially Promoted Research, No. 18H05209 (E.Y.).

REFERENCES AND NOTES

1 M. M. Green, J.-W. Park, T. Sato, A. Teramoto, S. Lifson, R. L. B. Selinger, J. V. Selinger, *Angew. Chem. Int. Ed.* **1999**, *38*, 3138.

2 T. Nakano, Y. Okamoto, *Chem. Rev.* **2001**, *101*, 4013.

3 M. Suginome, Y. Ito, *Adv. Polym. Sci.* **2004**, *17*, 77.

4 M. Fujiki, *Chem. Rec.* **2009**, *9*, 271.

5 E. Yashima, K. Maeda, H. Iida, Y. Furusho, K. Nagai, *Chem. Rev.* **2009**, *109*, 6102.

6 R. M. Ho, Y. W. Chiang, S. C. Lin, C. K. Chen, *Prog. Polym. Sci.* **2011**, *36*, 376.

7 E. Schwartz, M. Koepf, H. J. Kitto, R. J. M. Nolte, A. E. Rowan, *Polym. Chem.* **2011**, *2*, 33.

8 E. Yashima, N. Ousaka, D. Taura, K. Shimomura, T. Ikai, K. Maeda, *Chem. Rev.* **2016**, *116*, 13752.

9 R. J. M. Nolte, A. J. M. Van Beijnen, W. Drenth, *J. Am. Chem. Soc.* **1974**, *96*, 5932.

10 H. Yuki, Y. Okamoto, I. Okamoto, *J. Am. Chem. Soc.* **1980**, *102*, 6356.

11 E. Yashima, S. Huang, Y. Okamoto, *J. Chem. Soc. Chem. Commun.* **1994**, 1811.

12 C. Zhang, F. Liu, Y. Li, X. Shen, X. Xu, R. Sakai, T. Satoh, T. Kakuchi, Y. Okamoto, *J. Polym. Sci. Part A: Polym. Chem.* **2013**, *51*, 2271.

13 K. Shimomura, T. Ikai, S. Kanoh, E. Yashima, K. Maeda, *Nat. Chem.* **2014**, *6*, 429.

14 K. Maeda, M. Maruta, K. Shimomura, T. Ikai, S. Kanoh, *Chem. Lett.* **2016**, *45*, 1063.

15 J. Shen, Y. Okamoto, *Chem. Rev.* **2016**, *116*, 1094.

16 T. Ikai, S. Awata, T. Kudo, R. Ishidate, K. Maeda, S. Kanoh, *Polym. Chem.* **2017**, *8*, 4190.

17 D. Hirose, A. Isobe, E. Quiñoá, F. Freire, K. Maeda, *J. Am. Chem. Soc.* **2019**, *141*, 8592.

18 E. Yashima, K. Maeda, T. Nishimura, *Chem. A Eur. J.* **2004**, *10*, 42.

19 E. Yashima, K. Maeda, *Macromolecules* **2008**, *41*, 3.

20 M. Fujiki, *Symmetry* **2014**, *6*, 677.

21 K. Maeda, E. Yashima, *Top. Curr. Chem.* **2017**, *375*, 72.

22 S. Fukao, M. Fujiki, *Macromolecules* **2009**, *42*, 8062.

23 K. Suda, K. Akagi, *Macromolecules* **2011**, *44*, 9473.

24 D. Lee, Y.-J. Jin, H. Kim, N. Suzuki, M. Fujiki, T. Sakaguchi, S. K. Kim, W.-E. Lee, G. Kwak, *Macromolecules* **2012**, *45*, 5379.

25 Y. Nagata, T. Nishikawa, M. Suginome, *Chem. Commun.* **2014**, *50*, 9951.

26 T. Ikai, S. Shimizu, S. Awata, T. Kudo, T. Yamada, K. Maeda, S. Kanoh, *Polym. Chem.* **2016**, *7*, 7522.

27 K. Maeda, M. Maruta, Y. Sakai, T. Ikai, S. Kanoh, *Molecules* **2016**, *21*, 1487.

28 R. P. Megens, G. Roelfes, *Chem. A Eur. J.* **2011**, *17*, 8514.

29 M. Suginome, T. Yamamoto, Y. Nagata, T. Yamada, Y. Akai, *Pure Appl. Chem.* **2012**, *84*, 1759.

30 M. Suginome, T. Yamamoto, Y. Nagata, *J. Synth. Org. Chem. Jpn.* **2015**, *73*, 1141.

31 E. Yashima, Y. Maeda, Y. Okamoto, *Polym. J.* **1999**, *31*, 1033.

32 F. Sanda, H. Araki, T. Masuda, *Chem. Lett.* **2005**, *34*, 1642.

33 Z. Tang, H. Iida, H.-Y. Hu, E. Yashima, *ACS Macro Lett.* **2012**, *1*, 261.

34 L. Liu, Q. Long, T. Aoki, G. Zhang, T. Kaneko, M. Teraguchi, C. Zhang, Y. Wang, *Chirality* **2015**, *27*, 454.

35 C. Zhang, Y. Qiu, S. Bo, F. Wang, Y. Wang, L. Liu, Y. Zhou, H. Niu, H. Dong, T. Satoh, *J. Polym. Sci. Part A: Polym. Chem.* **2019**, *57*, 1024.

36 M. Reggelin, M. Schultz, M. Holbach, *Angew. Chem. Int. Ed.* **2002**, *41*, 1614.

37 M. Reggelin, S. Doerr, M. Klussmann, M. Schultz, M. Holbach, *Proc. Natl. Acad. Sci. U. S. A.* **2004**, *101*, 5461.

38 C. A. Müller, T. Hoffart, M. Holbach, M. Reggelin, *Macromolecules* **2005**, *38*, 5375.

39 T. Miyabe, Y. Hase, H. Iida, K. Maeda, E. Yashima, *Chirality* **2009**, *21*, 44.

40 L. Zhou, B.-F. Chu, X.-Y. Xu, L. Xu, N. Liu, Z.-Q. Wu, *ACS Macro Lett.* **2017**, *6*, 824.

41 L. Shen, L. Xu, X.-H. Hou, N. Liu, Z.-Q. Wu, *Macromolecules* **2018**, *51*, 9547.

42 T. Yamamoto, M. Suginome, *Angew. Chem. Int. Ed.* **2009**, *48*, 539.

43 T. Yamamoto, R. Murakami, M. Suginome, *J. Am. Chem. Soc.* **2017**, *139*, 2557.

44 T. Yamamoto, R. Murakami, S. Komatsu, M. Suginome, *J. Am. Chem. Soc.* **2018**, *140*, 3867.

45 Y. Okamoto, K. Suzuki, K. Ohta, K. Hatada, H. Yuki, *J. Am. Chem. Soc.* **1979**, *101*, 4763.

46 E. Yashima, K. Maeda, Y. Okamoto, *Nature* **1999**, *399*, 449.

47 K. Maeda, K. Morino, Y. Okamoto, T. Sato, E. Yashima, *J. Am. Chem. Soc.* **2004**, *126*, 4329.

48 T. Miyagawa, A. Furuko, K. Maeda, H. Katagiri, Y. Furusho, E. Yashima, *J. Am. Chem. Soc.* **2005**, *127*, 5018.

49 Y. Nagata, R. Takeda, M. Suginome, *ACS Cent. Sci.* **2019**, *5*, 1235.

50 R. Ishidate, A. J. Markvoort, K. Maeda, E. Yashima, *J. Am. Chem. Soc.* **2019**, *141*, 7605.

51 M. Nakajima, M. Saito, M. Shiro, S. Hashimoto, *J. Am. Chem. Soc.* **1998**, *120*, 6419.

52 B. Bai, H.-J. Zhu, W. Pan, *Tetrahedron* **2012**, *68*, 6829.

53 T. Shimada, A. Kina, S. Ikeda, T. Hayashi, *Org. Lett.* **2002**, *4*, 2799.

54 K. Maeda, D. Hirose, N. Okoshi, K. Shimomura, Y. Wada, T. Ikai, S. Kanoh, E. Yashima, *J. Am. Chem. Soc.* **2018**, *140*, 3270.

55 S. Sakurai, K. Okoshi, J. Kumaki, E. Yashima, *Angew. Chem. Int. Ed.* **2006**, *45*, 1245.

56 S. Sakurai, K. Okoshi, J. Kumaki, E. Yashima, *J. Am. Chem. Soc.* **2006**, *128*, 5650.

57 S. Sakurai, S. Ohsawa, K. Nagai, K. Okoshi, J. Kumaki, E. Yashima, *Angew. Chem. Int. Ed.* **2007**, *46*, 7605.

58 J. Kumaki, S. Sakurai, E. Yashima, *Chem. Soc. Rev.* **2009**, *38*, 737.

59 K. Maeda, H. Mochizuki, M. Watanabe, E. Yashima, *J. Am. Chem. Soc.* **2006**, *128*, 7639.

60 K. Maeda, K. Shimomura, T. Ikai, S. Kanoh, E. Yashima, *Macromolecules* **2017**, *50*, 7801.

61 A nearly perfect control of the macromolecular helicity memorized in $hm_{(R)5}$-poly-**2b** and $hm_{(R)35}$-poly-**2b** was confirmed by the facts that their dissymmetry factor (g_{abs}) values, defined as $g_{abs} = \Delta\varepsilon/\varepsilon$, measured in toluene at −10 °C ($+5.8 \times 10^{-3}$ at 383 nm and -5.4×10^{-3} at 381 nm, respectively) were virtually the same to those of complete left- ($+5.7 \times 10^{-3}$ at 383 nm) and right-handed (-5.7×10^{-3} at 383 nm) helical poly(biphenylylacetylene)s carrying optically pure ((*R*) or (*S*)) pendant groups measured in toluene at −10 °C, respectively.[50]

62 It is well known that the catalytic activity and enantioselectivity of pyridine *N*-oxide-based chiral organocatalysts for asymmetric allylation of benzaldehydes are significantly dependent on the structures of the chiral organocatalysts and solvents.[63,64] In general, polar dichloromethane and acetonitrile, which are commonly used as the solvents, tend to give better catalytic activities and higher enantioselectivities toward asymmetric allylation of benzaldehydes than in nonpolar toluene used in the present study.

63 G. Chelucci, G. Murineddu, G. A. Pinna, *Tetrahedron Asymmetry* **2004**, *15*, 1373.

64 M. Yus, J. C. González-Gómez, F. Foubelo, *Chem. Rev.* **2011**, *111*, 7774.

65 R. Hrdina, M. Dračínský, I. Valterová, J. Hodačová, I. Císařová, M. Kotora, *Adv. Synth. Catal.* **2008**, *350*, 1449.